Intermittency of near-bottom turbulence in tidal flow on a shallow shelf

I. Lozovatsky,[1,2] E. Roget,[3] J. Planella,[3] H. J. S. Fernando,[1] and Zhiyu Liu[4]

Received 12 February 2009; revised 22 September 2009; accepted 20 November 2009; published 11 May 2010.

[1] The higher-order structure functions of vertical velocity fluctuations (transverse structure functions (TSF)) were employed to study the characteristics of turbulence intermittency in a reversing tidal flow on a 19 m deep shallow shelf of the East China Sea. Measurements from a downward-looking, bottom-mounted Acoustic Doppler Velocimeter, positioned 0.45 m above the seafloor, which spanned two semidiurnal tidal cycles, were analyzed. A classical lognormal single-parameter (μ) model for intermittency and the universal multifractal approach (specifically, the two-parameter (C_1 and α) log-Levy model) were employed to analyze the TSF exponent $\xi(q)$ in tidally driven turbulent boundary layer and to estimate μ, C_1, and α. During the energetic flooding tidal phases, the parameters of intermittency models approached the mean values of $\widetilde{\mu} \approx 0.24$, $\widetilde{C}_1 \approx 0.15$, and $\widetilde{\alpha} \approx 1.5$, which are accepted as the universal values for fully developed turbulence at high Reynolds numbers. With the decrease of advection velocity, μ and C_1 increased up to $\mu \approx 0.5$–0.6 and $C_1 \approx 0.25$–0.35, but α decreased to about 1.4. The results explain the reported disparities between the smaller "universal" values of intermittency parameters μ and C_1 (mostly measured in laboratory and atmospheric high Reynolds number flows) and those ($\mu = 0.4$–0.5) reported for oceanic stratified turbulence in the pycnocline, which is associated with relatively low local Reynolds numbers $R_{\lambda w}$. The scaling exponents $\xi(2)$ of the second-order TSF, relative to the third-order structure function, was also found to be a decreasing function of $R_{\lambda w}$, approaching the classical value of 2/3 only at very high $R_{\lambda w}$. A larger departure from the universal turbulent regime at lower Reynolds numbers could be attributed to the higher anisotropy and associated intermittency of underdeveloped turbulence.

Citation: Lozovatsky, I., E. Roget, J. Planella, H. J. S. Fernando, and Z. Liu (2010), Intermittency of near-bottom turbulence in tidal flow on a shallow shelf, *J. Geophys. Res.*, *115*, C05006, doi:10.1029/2009JC005325.

1. Introduction

[2] By its very nature, turbulence in geophysical flows is highly intermittent in space and time. Turbulence characteristics such as the kinetic energy e_{tr}, its dissipation ε, eddy diffusivities K, scalar dissipation χ, turbulent scales L_{tr} are subjected to sharp variations with typical spatial scales of tens/hundreds meters vertically/horizontally and temporal scales ranging from minutes to hours. Such mesoscale inhomogeneity of hydrophysical fields is called "external or outer intermittency," and is associated with variations of mean fields, patchiness of turbulent regions and presence of interfaces that separate turbulent and nonturbulent regions [*Sreenivasan*, 2004]. Conversely, the small-scale, fine-scale intermittency of turbulence or internal intermittency occurs at spatial scales from meters to millimeters, and is usually confined within turbulent regions (layers, patches, wakes, plumes, etc.). It is attributed to random inhomogeneous spatial distribution of vortex filaments within turbulent regions, where they stretch and dissipate energy in isolation [*Kuo and Corrsin*, 1971].

[3] Mesoscale intermittency is a phenomenon characteristic of turbulent mixing in oceans, seas, large lakes and reservoirs, which may not be observed in other turbulent flows. The measured vertical and horizontal sizes of turbulent zones in the upper ocean are subjected to specific statistical regularities. Their probability distributions appear to be approximately lognormal while the distances between turbulent regions follow a double exponential distribution [*Lozovatsky et al.*, 1993; *Pozdinin*, 2002]. Internal intermittency, however, is inherent to any high Reynolds number turbulent flow [*Monin and Yaglom*, 1975] due to its inhomogeneous microstructure.

[1]Center for Environmental Fluid Dynamics, Department of Mechanical and Aerospace Engineering, Arizona State University, Tempe, Arizona, USA.
[2]Catalan Institute for Water Research, Girona, Spain.
[3]Environmental Physics Group, Department of Physics, University of Girona, Girona, Spain.
[4]State Key Laboratory of Marine Environmental Science, Xiamen University, Xiamen, China.

0148-0227/10/2009JC005325

[4] Internal intermittency of turbulence in oceans and lakes affects processes at the scales of inertial-convective and diffusive subranges [*Tennekes and Lumley*, 1972]. Among them are the viscous dissipation of energy, biochemical processes (planktonic mating, predator-prey contacts, chemical reactions [*Seuront and Schmitt*, 2005]), thermal convection and redistribution of salinity concentration or multi/double diffusive convective fluxes [*Sánchez and Roget*, 2007]. The influence of small-scale turbulent fluctuations on the propagation of light and sound in the ocean is an important problem for various applications of ocean optics and acoustics [*Tyson*, 1991; *Colosi et al.*, 1999].

[5] In application to aquatic ecosystems, turbulent oscillations of various scales influence aggregation, incubation and foraging processes of small-scale planktonic organisms [*Druet*, 2003]. Internal intermittency can affect phyto and zooplankton species less than several millimeters in size [*Peters and Marrasé*, 2000], specifically, floating microscopic algae that are responsible for photosynthesis in coastal oceans [*Margalef*, 1985, 1997]. Zooplankton larger than ~1 cm usually do not react to small-scale intermittency of turbulence [*Squires and Yamazaki*, 1995, 1996].

[6] Intermittency of biochemical (plankton, nitrites) and scalar (fluorescence concentration, temperature) variables have been studied by Seuront and coauthors in a series of papers [e.g., *Seuront et al.*, 1999, 2001, 2002; *Seuront and Schmitt*, 2005]. In particular, it was found that phytoplankton patchiness substantially increased the predator-prey encounter rates, but the encounter was much less influenced by turbulence when ε was considered as an intermittent variable rather than a mean value [*Seuront et al.*, 2001]. The patchiness of small-scale phytoplankton distribution in a tidal current (the Eastern English Channel) increased with decreasing turbulence intensity [*Seuront and Schmitt*, 2005] and it varied depending on the phase of tidal cycle. This finding is directly consistent with the present results.

[7] The first results on intermittency of ocean turbulence at scales of inertial-convective subrange, with application to scalar dissipation χ, were presented by *Fernando and Lozovatsky* [2001] and for the velocity field and ε by *Seuront and Schmitt* [2001] and *Yamazaki et al.* [2006]. *Seuront and Schmitt* [2001] concluded that fluorescence is more intermittent than the velocity, but less intermittent than the conductivity fields in the Neko Seto Sea, offshore the Japanese coast. The distributions of ε and χ in deep ocean and shallow waters, at the scales from tens of centimeters to several meters that are affected by internal as well as external intermittencies, were found to be approximately lognormal [e.g., *Baker and Gibson*, 1987; *Gibson*, 1991; *Gregg et al.*, 1993; *Rehmann and Duda*, 2000; *Lozovatsky and Fernando*, 2002; *Lozovatsky et al.*, 2006; *Yamazaki and Lueck*, 1990; *Davis*, 1996], but they disputed the applicability of lognormal approximation to the distribution of ε in the ocean.

[8] Most theoretical studies on internal intermittency (see reviews of *Lesieur* [1990], *Frisch* [1995], and *Seuront et al.* [2005]) employed a suite of scaling models, either of the fluctuations of ε_r or qth-order statistical moments of velocity increments $\langle \Delta V_r^q \rangle$, which are also called the qth-order structure functions (SF). The angle brackets indicate ensemble averaging over a specific volume in the inertial subrange with a characteristic radius r. Laboratory experiments, DNS, and atmospheric measurements have produced voluminous literature on internal intermittency (see reviews of *Sreenivasan and Antonia* [1997], *Anselmet et al.* [2001], *Tsinober* [2001], *Vassilicos* [2001], *Seuront et al.* [2005], and *Lovejoy and Schertzer* [2007]). Specific findings of previous theoretical and laboratory studies will be given in sections 5 and 6 in relation to our results.

[9] In all, despite recent progress, small-scale intermittency within turbulent patches of the pycnocline or in the surface and bottom boundary layers has not been extensively studied and remains a relatively unexplored area in physical oceanography, though its oceanic applications abound. The goal of this paper is to investigate internal intermittency of marine turbulence near the seabed during different phases of a nonstratified reversing tidal flow and determine whether the intermittency parameters depend on the boundary layer and microscale Reynolds numbers. The analysis is based on measurements of vertical velocity w using a bottom mounted Acoustic Doppler Velocimeter (ADV). An overview of the scaling concepts in relation to structure functions analysis is given in section 2. Section 3 contains a brief summary of the measurement site and its hydrography as well as averaged turbulence parameters. The data have already been analyzed for mean flow and tidally induced temporal variations of averaged dissipation rate and friction velocity [*Lozovatsky et al.*, 2008a, 2008b]. The methodology of the SF analysis and calculation of the scaling exponents of the transverse structure functions (TSF) as well as the dissipation rate are presented in section 4, followed by the results in section 5. This includes the evolution of basic turbulence parameters (section 5.1) and transverse structure function exponents (TSFE) during the tidal cycle (section 5.2), a comparison of scaling exponents with log-Levy and lognormal intermittency models (section 5.3) and a discussion of dynamical relevance of model parameters (section 5.4). The dependence of the second-order TSFE on microscale turbulent Reynolds number is presented (section 5.5). The possible influence of Taylor hypothesis on evaluating TSFE is addressed in section 6 as well as other sources of uncertainty that may affect results. Conclusions are given in section 7.

2. Structure Functions and Intermittency Models

[10] The wide range of scales of ocean processes affected by turbulent motions naturally calls for a scaling approach of studying intermittency of ocean turbulence. To paraphrase Landau on *Kolmogorov*'s [1941a] turbulent cascade, "… in a turbulent field the presence of curl of the velocity was confined to a limited region …" (cited by *Frisch* [1995]), which indicates the essence of turbulence intermittency. To account for fluctuations of ε (and χ) at the scales r of locally isotropic turbulence in inertial-convective and viscous spectral subranges, *Kolmogorov* [1962] and *Oboukhov* [1962] suggested a refined similarity hypothesis (RSH). It argues that the velocity increment ΔV_r over a separation distance r is specified not by the mean dissipation rate $\widetilde{\varepsilon}$ but the dissipation ε_r averaged over a specific volume of radius $r < L_o$, which leads to the following scaling relation

$$\Delta V_r \sim (\varepsilon_r r)^{1/3}, \tag{1a}$$

where L_o is an external turbulent scale and ΔV_r is the increment of any component (u, v or w) of velocity fluctuations in the longitudinal (x) and transverse (y) and (z) directions, respectively. Accordingly, the qth-order velocity increment

$$\Delta V_r^q \sim \varepsilon_r^{q/3} r^{q/3}. \tag{1b}$$

The probability distribution of ε_r was considered lognormal, which is based on *Kolmogorov*'s [1941b] postulate that the sizes of particles resulting from a series of successive statistically independent breaking must be asymptotically lognormal. *Yaglom* [1966] and *Gurvich and Yaglom* [1967] theoretically derived an explicit cascade intermittency model, wherein transfer of kinetic energy down the cascade occurs with the breakdown of turbulent eddies, which produce lognormally distributed ε_r with the variance

$$\sigma^2_{\log \varepsilon_r} = A_\varepsilon + \mu \log\left(\frac{L_\circ}{r}\right), \tag{2a}$$

where A_ε depends on the large-scale motions and μ is an intermittency factor that accounts for stretching of the probability distribution function of log ε_r [e.g., *Monin and Yaglom*, 1975; *Frisch*, 1995].

[11] For the scalar dissipation rate χ_r (e.g., fluctuations of temperature, conductivity, fluorescence concentration) [*Gibson*, 1981]

$$\sigma^2_{\log \chi_r} = A_\chi + \mu^{sc} \log\left(\frac{L_\circ}{r}\right), \tag{2b}$$

where μ^{sc} is the intermittency factor of the scalars corresponding to χ_r and A_χ depend on the characteristics of mean flow. Both intermittency factors μ and μ^{sc} are assumed universal, with canonical values $\mu \approx 0.25$ and $\mu^{sc} \approx 0.35$ for very high Reynolds number turbulence, with μ^{sc} having lesser statistical confidence than μ [*Sreenivasan and Kailasnath*, 1993].

[12] The lognormal model of intermittency led to the modification of Kolmogorov-Oboukhov original scaling (the −5/3 laws for the spectral densities and 2/3 laws for the second-order structure functions) by small additives $\mu/9$ and $\mu^{sc}/9$. The modified spectral functions are [*Monin and Yaglom*, 1975]

$$E_u(\kappa) = c_K \varepsilon_r^{2/3} \kappa^{-5/3+\mu/9} \quad \text{and} \quad E_{sc}(\kappa) = c_{sc} \chi_r \varepsilon_r^{-1/3} \kappa^{-5/3+\mu^{sc}/9}, \tag{3}$$

where c_K and c_{sc} are universal constants. Equations (2a) and (2b) have been utilized for empirical estimation of μ and μ^{sc} in laboratory experiments [e.g., *Gibson et al.*, 1970] and for ocean turbulence. For mesoscale intermittency, μ and μ^{sc} ranged between 0.44 and 0.5 (see review of *Gibson* [1998]). The same numbers ($\mu^{sc} = 0.44$) were obtained by *Fernando and Lozovatsky* [2001] by analyzing microstructure of oceanic conductivity (temperature) in the thermocline. Although the lognormal model of intermittency is simple and convenient, as discussed by *Novikov* [1970, 1990], *Frisch* [1995], and *Seuront et al.* [2005], it is mathematically ill posed.

[13] The application of multifractal theory [*Mandelbrot*, 1974] to study turbulence was the next important step for understanding and quantifying the multiscale nature of the intermittency phenomenon. The cascade of energy flux can be thought of as a multiplicative process where larger eddies are randomly modulated by smaller eddies to determine the fraction of energy transfer from larger to smaller scales [*Seuront and Schmitt*, 2005], which naturally entertains a multifractal approach as a tool. This approach associates each intermittency level p_r (a fraction of the volume L_o^3 occupied by turbulence of characteristic scale $r = \gamma^n L_o$, $0 < \gamma < 1$) with its own fractal dimension $D = \log N(n)/\log n$, where N is a number of self-similar structures and n^{-1} is a fraction (reduction) factor. In the simplest case of a β model [*Fournier and Frisch*, 1978], p_r is assumed to decrease at all levels by the same constant factor $0 < \beta < 1$, so that after n ($= \log(r/L_o)/\log\ \gamma$) breakdowns, $p_r = \beta^n = (r/L_o)^{3-D}$, where $3 - D = \log \beta/\log \gamma$ (see *Frisch* [1995, chapter 8] for details).

[14] The multifractal models are based on the scaling assumption that if $\varepsilon_r^{q/3}$ has a power law variation with r in the inertial subrange then all qth-order statistical moments of velocity increments (i.e., qth-order structure functions) can be written as

$$\left\langle \Delta V_r^q \right\rangle = C_q (\varepsilon_r r)^{\xi(q)}, \tag{4}$$

where the constant C_q may depend on large-scale flow characteristics. The exponent function $\xi(q)$ signifies the multiscale transfer process specified by statistical moments of order q. The scaling exponent, which is universal ($\xi(q) = q/3$) for nonintermittent Kolmogorov turbulence under very high local Reynolds numbers $r(\varepsilon_r r)^{1/3}/\nu$, is thought to be universal for intermittent turbulence whence ξ is a nonlinear function of q [*Sreenivasan and Antonia*, 1997].

[15] A number of models (see review of *Seuront et al.* [2005]) have been suggested to specify $\xi(q)$ in (4). Here we choose the log-Levy multifractal model [*Schertzer and Lovejoy*, 1987], since it has already been used in several oceanographic applications cited above. Note that the log-Levy model is stable under addition of the logarithm of the process variable [*Feller*, 1971; *Mandelbrot*, 1983]. For the scaling exponent $\xi(q)$ this model gives

$$\xi(q) \equiv \xi_{fm} = \frac{q}{3} - \frac{C_1}{\alpha - 1}\left[\left(\frac{q}{3}\right)^\alpha - \frac{q}{3}\right], \tag{5}$$

where C_1 and α reflect the multifractal nature of intermittency in point. *Seuront et al.* [2005] suggested that C_1 and α have universal values close to 0.15 and 1.5, respectively, for very high Reynolds numbers. The Levy distribution index $0 < \alpha < 2$ and the multifractal codimension of mean C_1 characterizes the intermittency of the turbulent field in a way that sparseness and variability of the localized events (singularities) increase with increasing C_1 and decreasing α. Note that in a d-dimensional space with fractal dimension D, the quantity d-D is called the codimension [*Frisch*,

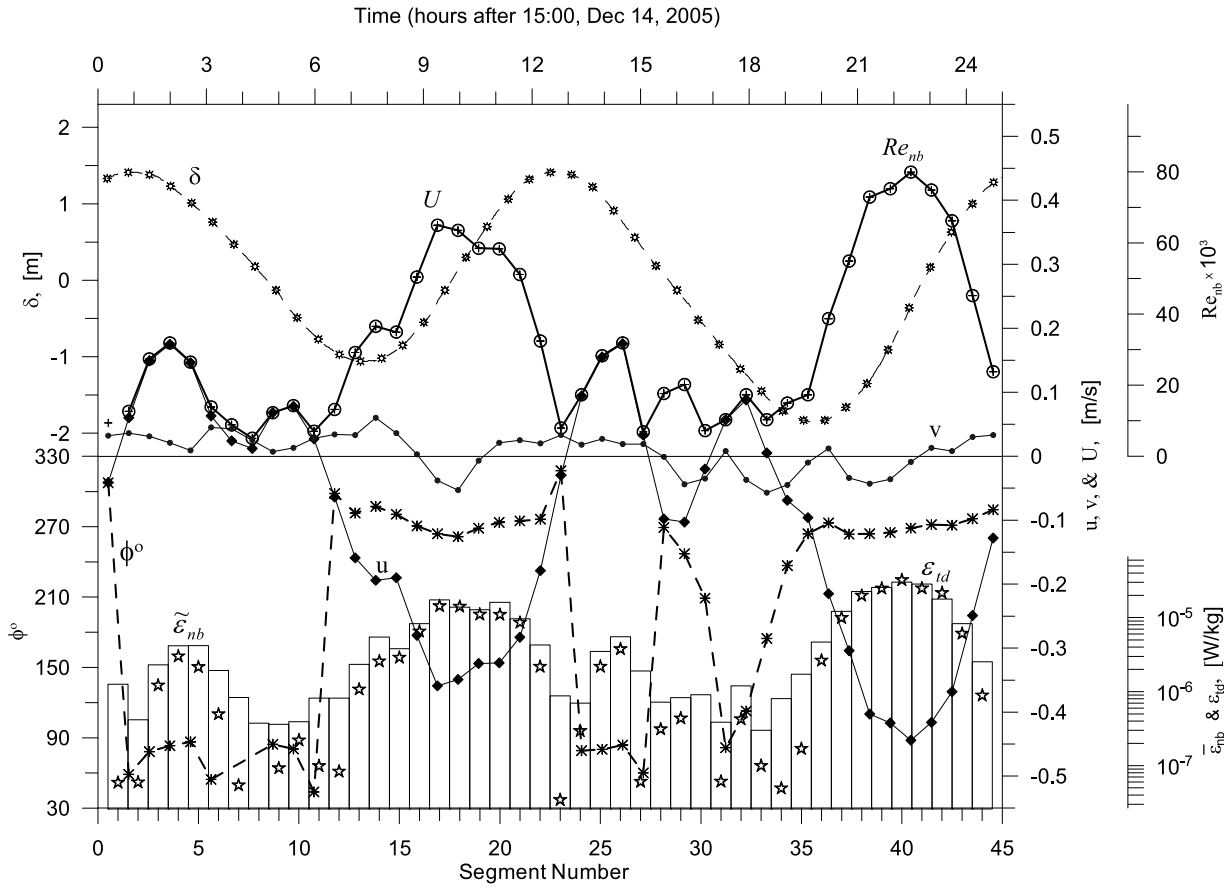

Figure 1. The surface elevation δ; the magnitude U; and direction ϕ^o of near-bottom current, its streamwise u and transverse v components. The segment-averaged "−5/3" dissipation rate $\widetilde{\varepsilon}_{nb}$ is represented by bars and the tidal dissipation ε_{td} is represented by stars. The near-bottom Reynolds number Re_{nb} (circles with crosses) coincides with the U curve.

1995]. For a quadratic polynomial function ($\alpha = 2$), equation (5) gives the scaling exponent for the lognormal intermittency model

$$\xi(q) \equiv \xi_{lm} = \frac{q}{3} - \frac{\mu}{18}\left(q^2 - 3q\right), \tag{6}$$

which has the same intermittency factor μ as in equation (2a).

3. Measurements and Background Hydrology

[16] The data taken in a shallow water tidal current, including a bottom-mounted Acoustic Doppler Velocimeter (ADV) measurements and hourly CTD profiles, were used in the study. The measurements were conducted on 14 December 2005, about 1.2 km offshore the northeastern coast of China (36.04°N, 120.32°E) at a water depth of 19 m. The measurement volume of a downward looking Nortek 6 MHz ADV "Vector" was set up at ζ_s = 0.45 m above the bottom for a 25 hour period, covering two complete semidiurnal tidal cycles. The ADV sampling rate was 16 Hz; the data were recorded continuously.

[17] A nearly unidirectional reversing tidal flow [*Lozovatsky et al.*, 2008a, Figure 6] dominated mesoscale dynamics at the test site (see also Figure 1). The M_2 amplitude of the west-directed flood current $u(t)$ of ~0.35–0.42 m/s was twice that of the eastern ebb current; the amplitude of transversal horizontal component $v(t)$ was much smaller ~0.05 m/s. The M_2 amplitude of surface elevation was 1.1 m. The reversing tidal flow was affected by seiches of ~2.3 hour period generated in the semienclosed Jiaozhou Bay located 2 km away. The seiching modulation of zonal velocity during the ebb tide was comparable with the tidal magnitude. The shallow water column was well mixed due to winter cooling from the sea surface and tidal mixing in the bottom boundary layer (BBL). The variations of the turbulent kinetic energy, averaged dissipation rate and friction velocity in the flow are given by *Lozovatsky et al.* [2008b].

4. Method

[18] To analyze the intermittency in tidal boundary layer turbulence, 25 hour records of the ADV current components were subdivided into 44 segments. Each segment contained 2^{15} = 32628 individual samples (time interval ~ 34 min), which is relatively long to provide sufficient multiplicative averaging of higher-order SF calculations (see section 4.2), thus minimizing errors to an acceptable level. On the other hand, turbulent fluctuations in the segments should be relatively stationary to yield reliable spectra and structure functions. Our tests showed that a 34 min segment is a good compromise between the above competing factors.

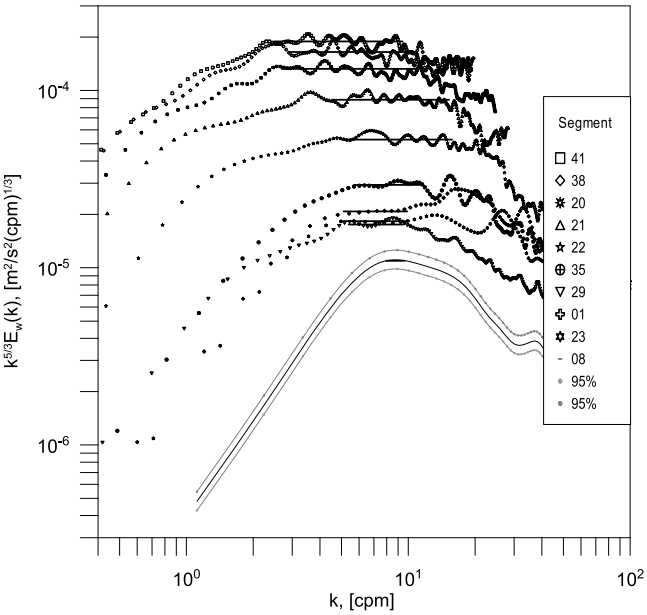

Figure 2. Examples of compensated spectral densities $k^{5/3}E_{w_i}(k)$. The spectra are arranged with respect to the near-bottom Reynolds number Re_{nb} from the highest (segment 41) to the lowest (segment 8). The inertial subranges are shown by horizontal lines. The 95% confident bounds (valid for every spectrum) are shown for the spectrum 8.

4.1. Spectra and the Dissipation Rate

[19] It is known [*Stapleton and Huntley*, 1995; *Voulgaris and Trowbridge*, 1998] that vertical velocity fluctuations w' obtained from a bottom-mounted ADV have a lower noise level at higher frequencies compared to those of u' and v'; this was also observed in our measurements. The spectral densities of all velocity components contained a relatively wide inertial subrange, and at frequencies $f > 3$–4 Hz the spectra of horizontal components were affected by noise while it was not the case for the spectra of the vertical component [*Lozovatsky et al.*, 2008b, Figure 2a]. Therefore, only the $w(t)$ records were used in further analysis.

[20] The mean dissipation $\widetilde{\varepsilon}_{nb}$ at each segment i (see Figure 1) was estimated from the inertial subranges of the frequency counterpart of the Kolmogorov wave number spectra

$$E_{w_i}(\kappa) = (U_i/2\pi)^{2/3} c_w \widetilde{\varepsilon}_{nb}^{2/3} f^{-5/3}, \tag{7}$$

with $c_w = 0.67$ [*Sreenivasan*, 1995] for one dimensional spanwise velocity spectrum and the magnitude of mean current $U_i = (\langle u\rangle_i^2 + \langle v\rangle_i^2)^{1/2}$. Several examples of the compensated $k^{5/3}E_{w_i}(k)$ spectra ($k = \kappa/2\pi$) are shown in Figure 2 for high, low, and intermediate Re_{nb}, where $Re_{nb} = (\Delta U/\zeta_s)L_{tr}^2/\nu$ is the near-bottom Reynolds number; here ΔU is the ADV velocity at ζ_s (thus, $U_{\zeta_{=0}} = 0$), ν the molecular viscosity, $L_{tr} = \kappa\zeta_s$ the characteristic turbulence scale above the seafloor, and κ the von Karman's constant. At each segment, the power spectral densities (PSD) were calculated using 1024 consecutive samples of w' with a 128-point spectral window and by further averaging PSD of 32 non-overlapping sections. Although the initial records $w_i(t)$ were quasi-stationary, they were detrended before spectral processing. The w measurements of ADV were of high quality [see *Lozovatsky et al.*, 2008a, 2008b], and thus the despiking procedure of *Goring and Nikora* [2002] was not used, which affects the signal structure.

[21] The inertial subrange of PSDs was typically well identifiable (Figure 2), which allowed investigations of "internal" intermittency using equations (5) and (6). At several segments, however, the −5/3 subrange was ill defined (e.g., segments 8, 24, and 30; an example is given in Figure 2), which were excluded from further analysis.

4.2. Calculation of the Structure Function Scaling Exponents

[22] The streamwise structure function of the vertical velocity (transverse SF or TSF) is defined as

$$s_i^q(r) \equiv \left\langle \Delta w_r^q \right\rangle = \overline{[w(x+r) - w(x)]^q}, \tag{8}$$

where x is the along-flow distance, $r = n(U_i/\Delta f)$ is the SF increment in the x direction, U_i is the magnitude of mean velocity at every segment (i = 1–44) containing 32628 samples each, $\Delta f = 16$ Hz the sampling frequency and n = 1, 2, … 32. Taylor's "frozen turbulence" hypothesis was employed to transform $w(t)$ at each segment to the spatial series $w(x)$. The applicability of Taylor's hypothesis was tested by calculating the ratio $rms_i(w')/U_i$; it never exceeded 2.5% at segments close to high and low tides (minimum advecting velocity) and mostly took values below 1%. Possible impacts of Taylor hypothesis on SF exponents is further addressed in section 5.

[23] Periods close to high and low tides (low Re_{nb}) showed a narrow inertial range (see Figure 2) and hence evaluation of $\xi(q)$ directly from the inertial-dissipative subrange of $s_i^q(r)$ could be subjected to substantial uncertainty. To overcome this problem, *Benzi et al.* [1993] suggested to scale the modulus of the qth-order SF not with respect to r, but with the modulus of the third-order structure function $|s^3(r)| \equiv S^3(r)$. It is known [*Kolmogorov*, 1941c] that for $r \gg \eta$, where $\eta = (\nu^3/\varepsilon)^{1/4}$ is the Kolmogorov scale, $S^3(r) \sim \varepsilon r$ is accurate and therefore $S_i^3(r)$ should not be affected by intermittency. In Figure 3, examples of $\log S_i^3(r)$ against $\log(r)$ are shown, and a wide "+1" subrange is evident for high Re_{nb} segments. This subrange almost disappears when Re_{nb} is low. Based on this rigorous result of the classic self-similarity theory, *Benzi et al.* [1993] argued that the velocity increment (Δw_r^q in our case) satisfies the equation

$$\langle |\Delta w(r)|^q \rangle = A_q \left| \left\langle \Delta w(r)^3 \right\rangle \right|^{\xi(q)} = B_q \left\langle |\Delta w(r)|^3 \right\rangle^{\xi(q)} \equiv S^q(r), \tag{9}$$

which is "… somehow more fundamental than the self-similar scaling with respect to r…" because it is valid even at moderate and low Reynolds numbers. Here A_q and B_q are two different sets of constants and the modulus accounts for the negative SF of odd orders. Equation (9) is sometimes referred to as the extended self-similarity, ESS [e.g., *Benzi et al.*, 1993, 1995; *van de Water and Herweijer*, 1999; *Hao et al.*, 2008]. The ESS allows for encompassing a wide scaling range even if the turbulence is not fully developed and the

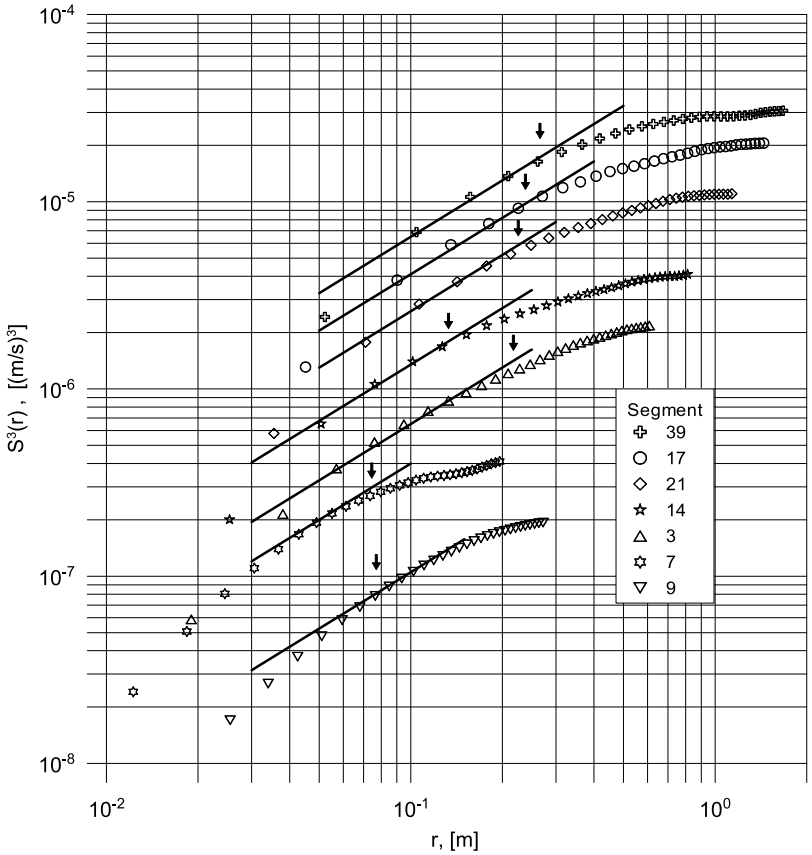

Figure 3. The third-order transverse structure functions for several segments. The "+1" subranges are highlighted by bold lines. The arrows correspond to the turbulent integral scale L_{int}.

separation between the dissipative and the integral turbulent scales is narrow (e.g., experiments of *Camussi et al.* [1996] (laboratory) and *Briscolini et al.* [1994] (numerical); also detailed discussions on this topic are given in these papers). Formally, it was suggested to plot log $S_i^q(r)$ versus log $S_i^3(r)$ instead of log(r). Such plots (Figures 4 and 5) show linear sections of SFs with good accuracy for moderate and low Re_{nb}; on the other hand, the inertial subrange in spectral densities was hardly detectable for the same Re_{nb}.

[24] The scaling $S_i^q(r)$ versus $S_i^3(r)$ was applied in the range $L_{int} > r > L_K$, where

$$L_{int} = c_o \left[rms\left(w'\right) \right]^3 / \widetilde{\varepsilon} \qquad (10)$$

is the integral turbulent scale and $L_K = c_{ds}\eta$ is the scale of maximum of dissipation. An approximate match between L_{int} and the low-wave number end of the inertial subrange in $E_w(\kappa)$ spectra was attained with $c_o = 0.6$. Although the constant c_{ds} that defines L_K could be as small as ~5–7 [*Gregg et al.*, 1996; *Camussi et al.*, 1996] or as large as 30 [*van de Water and Herweijer*, 1999], an intermediate estimate $c_{ds} = 15$ [*Monin and Yaglom*, 1975] was used to fit the $\log_{10} S_i^q(\log_{10} S_i^3)$ functions inside the inertial subrange, which did not necessarily cover all scales r. This also justifies the use of L_{int} and L_K in evaluating SF of all orders, although the inertial subrange of higher-order structure functions extends to smaller scales [*Frisch*, 1995].

[25] Our tests with high-order $S_i^q(r)$ ($q_{max} = 14$; $r_{max} = 32 \times U_i/\Delta f$) showed that a confident linear fit in the range $L_{int} > r > L_K$ can be applied to $\log_{10} S_i^q$ versus $\log_{10} S_i^3$ functions at almost all observational segments if $q < 7$–8. A few segments with the highest Re_{nb} (e.g., Figure 4) showed perfect linear fits for SF of much higher $q = 11$–12. To obtain confident scaling functions $\xi(q)$ for different tidal phases and evaluate intermittency models given by equations (5) and (6), $S_i^q(r)$ for all segments were calculated using the absolute values of streamwise increments of vertical velocity $\langle|\Delta w_r^q|\rangle$ for $q = 1$–7 in the r range (1–32) $\times$ $U_i/\Delta f$. Note that final estimates of $S_i^q(r)$ at the largest separation scale were obtained by averaging more than 1000 individual samples of $\Delta w'(r)$, ensuring minimal statistical error of $S_i^q(r)$. Indeed, the error of the seventh-order SF after averaging is equal to the error σ_w of an individual original sample of w, namely $7\sigma_w\sqrt{2/10^3} \approx \sigma_w$. Several examples of $S_i^q(r)$ versus $S_i^3(r)$ are shown in Figure 5, which exhibit clear linear sections (solid circles) in $\log_{10}$ scale. Scaling exponents $\xi(q)$ for every segment were determined by the least squares fits applied to these sections.

5. Results

5.1. Basic Characteristics of Turbulence Near the Seafloor

[26] The averaged kinetic energy dissipation rate near the bottom $\widetilde{\varepsilon}_{nb}$ (spectral estimates, equation (7)) generally

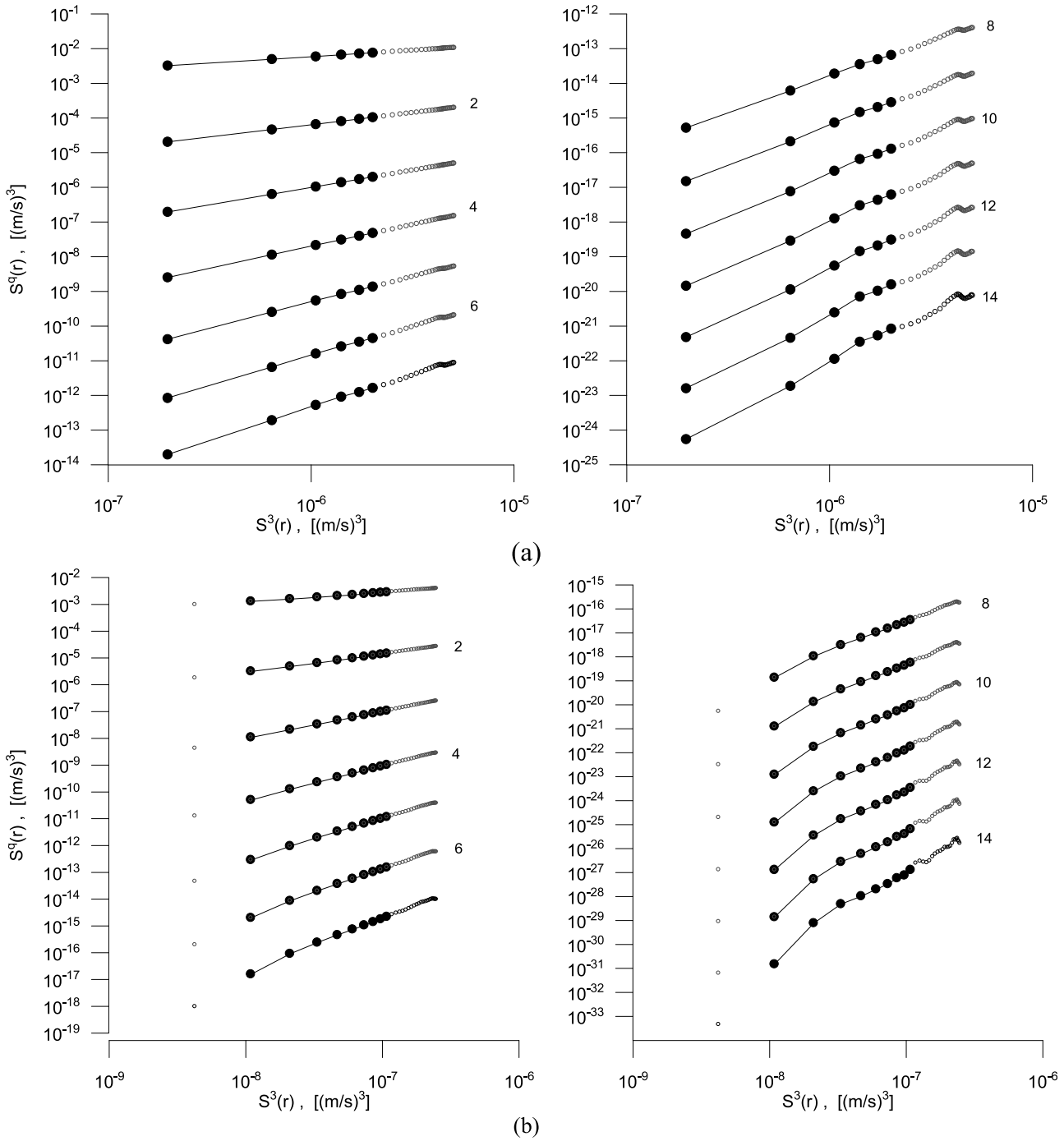

Figure 4. Examples of TSF plots showing $S_i^q(r)$ versus $S_i^3(r)$ for relatively (a) high $Re_{nb} \sim 4 \times 10^4$ (segment 36) and (b) low $Re_{nb} \sim 7 \times 10^3$ (segment 11). The numbers near the curves (2, …, 14) designate the even order TSFs. The range $L_{int} > r > L_K$ is highlighted by solid circles. The linear sections of the structure functions (in $\log_{10}$-$\log_{10}$ scale) are well defined up to q = 11–12 in Figure 4a but only up to q = 7–8 in Figure 4b.

followed the mean flow magnitude U, which specified the near-bottom Reynolds number Re_{nb} in the range 5×10^3 – 8×10^4 (see time variations of $\widetilde{\varepsilon}_{nb}$, U, and Re_{nb} in Figure 1). The highest $\widetilde{\varepsilon}_{nb} = 3 \times 10^{-5}$ W/kg was associated with tidal flooding and the lowest with ebbing. The periodic modulation of $\langle \varepsilon_{nb} \rangle$ during the ebb tide with a period of ~2 hours was consistent with seiching in the nearby Jiaozhou Bay [*Lozovatsky et al.*, 2008a]. The near-bottom diffusivity $K_{nb} = \widetilde{\varepsilon}_{nb}^{1/3} L_{tr}^{4/3}$ was ~$3 \times (10^{-4} – 10^{-3})$ m^2/s [*Lozovatsky et al.*, 2008b], which is about an order of magnitude larger than that observed on nontidal shelves [*Lozovatsky and Fernando*, 2002; *Roget et al.*, 2006].

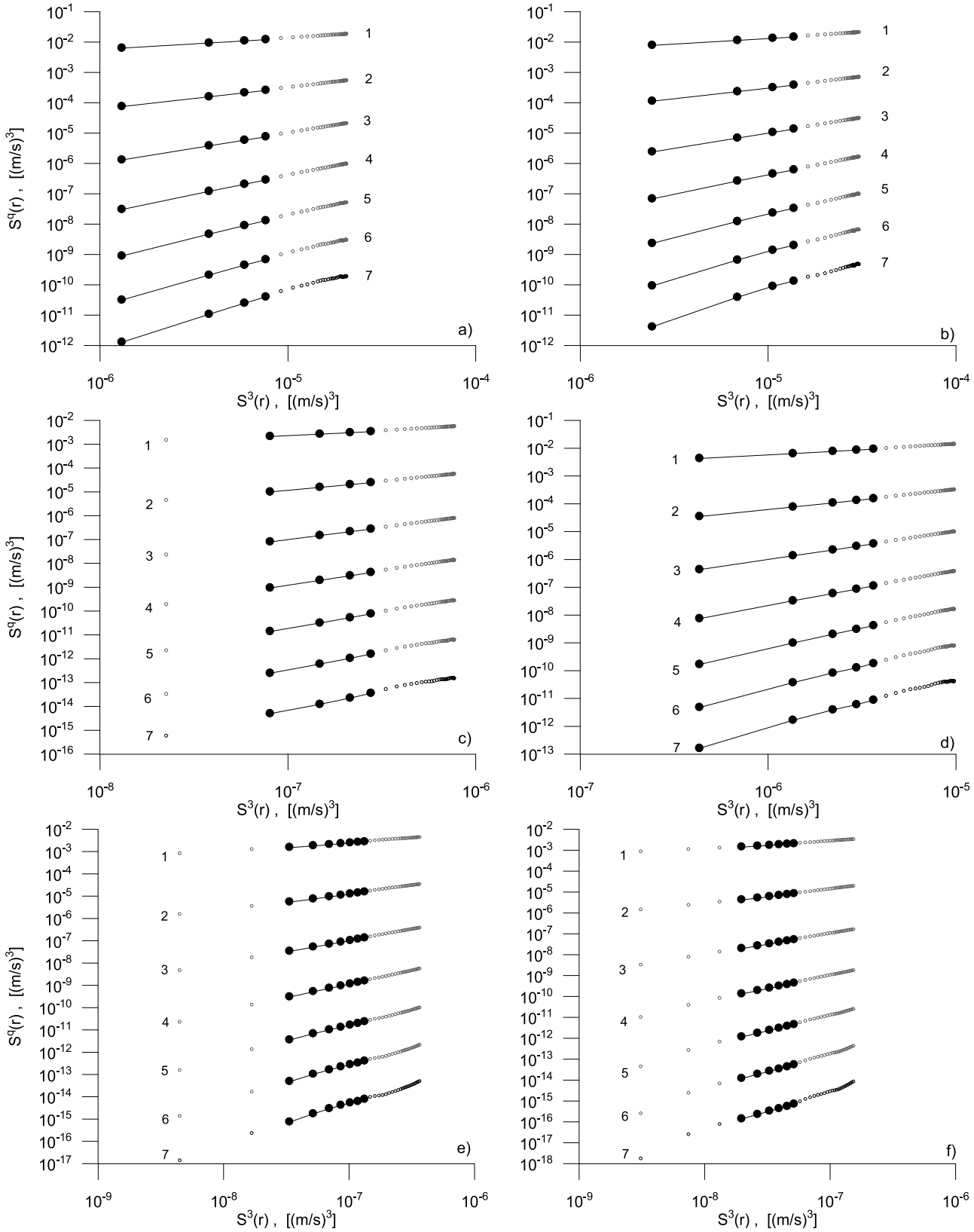

Figure 5. Examples of TSF plots showing $S_i^q(r)$ versus $S_i^3(r)$ (q = 1–7) for segments with high ((a) 17 and (b) 39), moderate ((c) 35 and (d) 43), and low ((e) 23 and (f) 33) Re_{nb}. The linear sections (in $\log_{10}$-$\log_{10}$ scale) are well defined and coincide with $L_{int} > r > L_K$ range highlighted by solid circles.

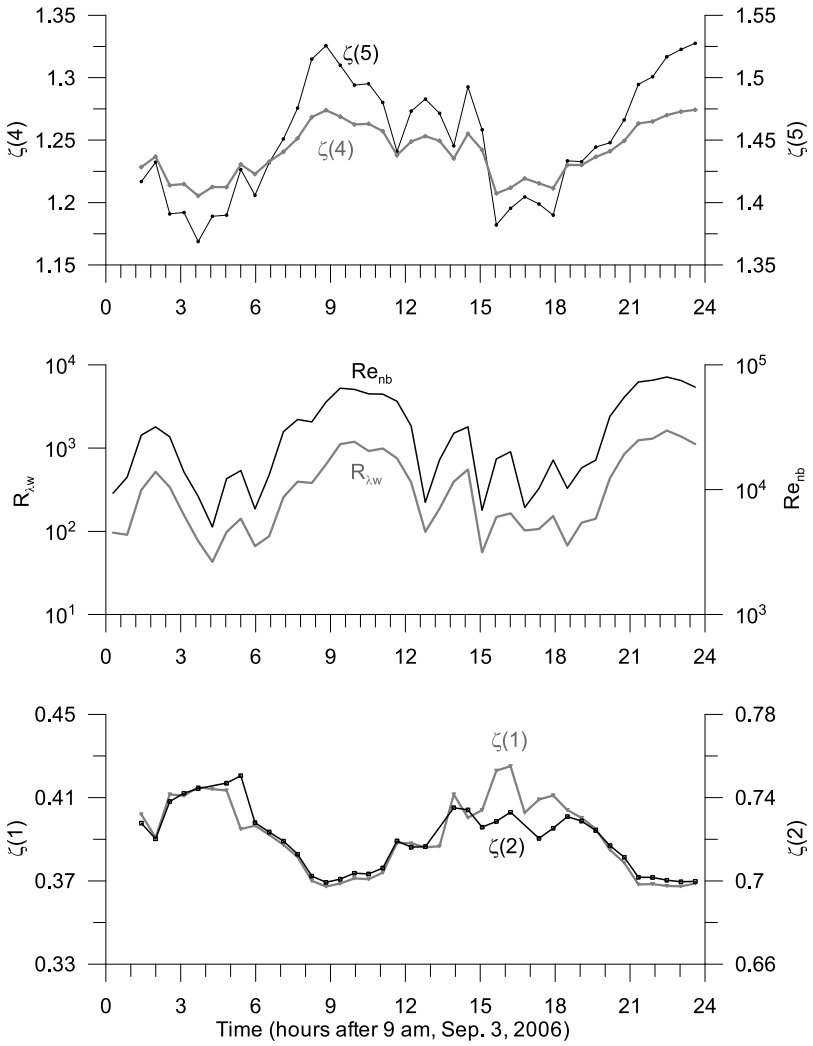

Figure 6. The running averaged estimates of the scaling exponents $\zeta(q)$ for (bottom) q = 1, 2 and (top) q = 4, 5, and (middle) the near-bottom (Re_{nb}) and local microscale ($R_{\lambda w}$) Reynolds numbers; note $\zeta(3) = 1$.

[27] The tidal dissipation rate $\varepsilon_{td} = c_{td}U_{bt}^3/\overline{H}$, which is also shown in Figure 1, was calculated using the barotropic tidal velocity U_{bt} (ADCP data) and the mean water depth $\overline{H}$ = 19 m [*MacKenzie and Leggett*, 1993]. The constant $c_{td} \approx 0.003$ that needed to match the spectral estimates of $\widetilde{\varepsilon}_{nb}$ in Figure 1 was two times smaller than that (0.006) of *Bowers and Simpson* [1987]. The correspondence between $\widetilde{\varepsilon}_{nb}$ and ε_{td} is especially good during two periods ($6.5 < t <$ 12.5 hours and $t >$ 20.5 hours) of almost unidirectional westerly ($\varphi \sim 270°$) flow with relatively high advection velocity (Figure 1).

[28] The turbulent kinetic energy e_{tr} and friction velocity u_* were calculated by *Lozovatsky et al.* [2008b] using the near-bottom ADV covariance measurements. It was found that the drag coefficient $C_d = u_*^2/U^2$ was approximately constant, with median value 1.65×10^{-3}. The classical parameterization of wall dissipation $\widetilde{\varepsilon}_{nb} = \frac{u_*^3}{\kappa\zeta}$ appeared to be valid as well as $\widetilde{\varepsilon}_{nb} = c_\varepsilon \frac{e_{tr}^{3/2}}{L_{tr}}$, with the constant c_s being close to the generally acceptable value of 0.08 [e.g., *Mellor and Yamada*, 1982; *Lozovatsky et al.*, 2006].

5.2. TSF Exponents in a Tidal Cycle

[29] The five-point running averaged estimates of $\xi(q$ = 1–5) are shown in Figure 6 ($\xi(3) = 1$ by definition). The exponents $\xi(1)$ and $\xi(2)$ are above the classical values 1/3 and 2/3, respectively, in all segments. The low-frequency variations of the first two scaling exponents (Figure 6 (bottom)) generally follow the tidal cycle, showing a decreasing trend as the tidal velocity increases and reaching maxima at $t \sim 9$ and 21 hours, corresponding to the maxima of Re_{nb} shown in Figure 6 (middle). The near-bottom Reynolds number R_{nb} was compared with the microscale turbulent Reynolds number

$$R_{\lambda w} = rms\left(w'\right)\lambda_w/\nu, \tag{11}$$

which is the major governing parameter for turbulence in the inertial-dissipative subrange [*Tennekes and Lumley*, 1972]. The $R_{\lambda w}$ is based on $rms(w')$ and the modified Taylor microscale

$$\lambda_w = \sqrt{\overline{(w')^2}/\overline{(dw'/dx)^2}}. \tag{12}$$

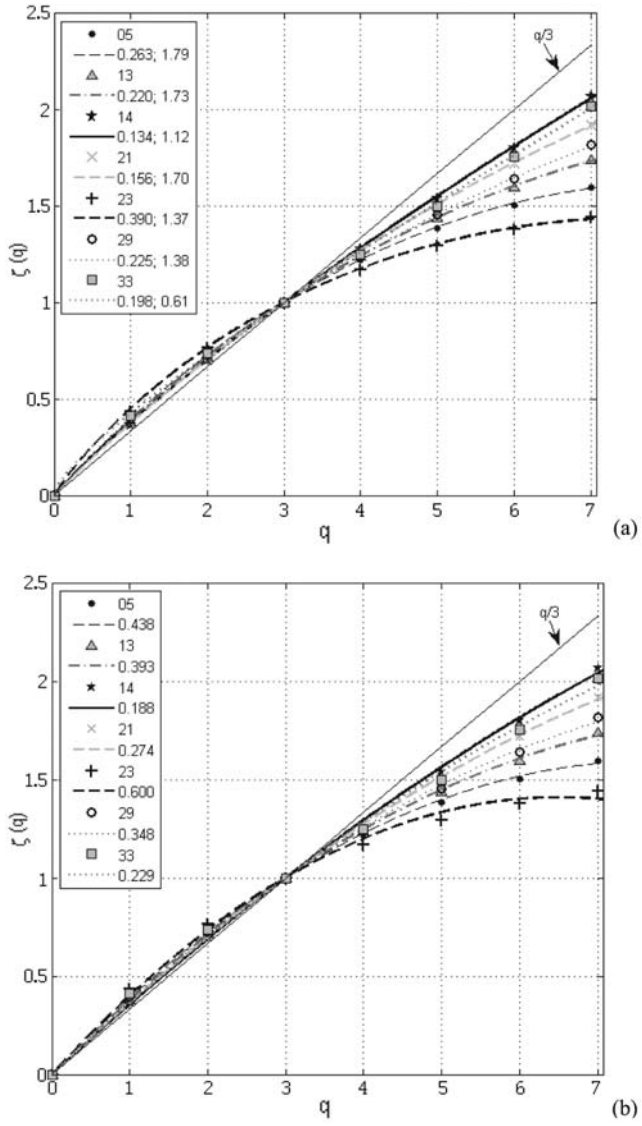

Figure 7. Examples of the empirical scaling exponents $\xi(q)$ for q = 1–7 at several segments (numbered in the insert) and their approximations by (a) the multifractal (equation (5)) and (b) lognormal (equation (6)) models. The symbols show empirical results and the lines show model predictions. The best-fit values of model parameters are given for each segment in the insets (C_1 and α in Figure 7a and μ in Figure 7b).

$R_{\lambda w}$ was selected over the conventional $R_\lambda = rms(u')\lambda/\nu$, where $\lambda = \sqrt{\overline{(u')^2}/\overline{(du'/dx)^2}}$ is the longitudinal Taylor microscale, because of the measurement accuracy considerations mentioned in section 4.2. The variations of $R_{\lambda w}$ almost mimic those of Re_{nb} (Figure 6 (middle)) suggesting a quasi-homogeneous energy cascade at scales between L_{tr} and λ_w.

[30] The higher-order exponents $\xi(4)$ and $\xi(5)$ are always below their classical values of 4/3 and 5/3, respectively, (Figure 6 (top)) but unlike $\xi(1)$ and $\xi(2)$ they show a growing trend with increasing Re_{nb} and $R_{\lambda w}$. This tendency is well correlated with the curvature of the empirical $\xi_i(q)$ functions that cross the classic $q/3$ curve at q = 3 (see Figures 7 and 8). A departure of $\xi_i(q)$ from the classical values appears to be pronounced at lower Re_{nb} (underdeveloped turbulence). In section 5.4, a physical interpretation of this tendency with decreasing $R_{\lambda w}$ is given.

5.3. Intermittency Parameters

[31] The scaling exponents $\xi_i(q)$ of TSF were approximated by equations (5) and (6) using the standard *cftool* utility of Matlab. The examples of $\xi_i(q)$ with respective multifractal (equation (5)) and lognormal (equation (6)) fits are shown in Figure 7 for representative segments. All empirical exponents $\xi_i(q)$ can be nicely fitted by equation (5) with a coefficient of determination above 0.98. In segments

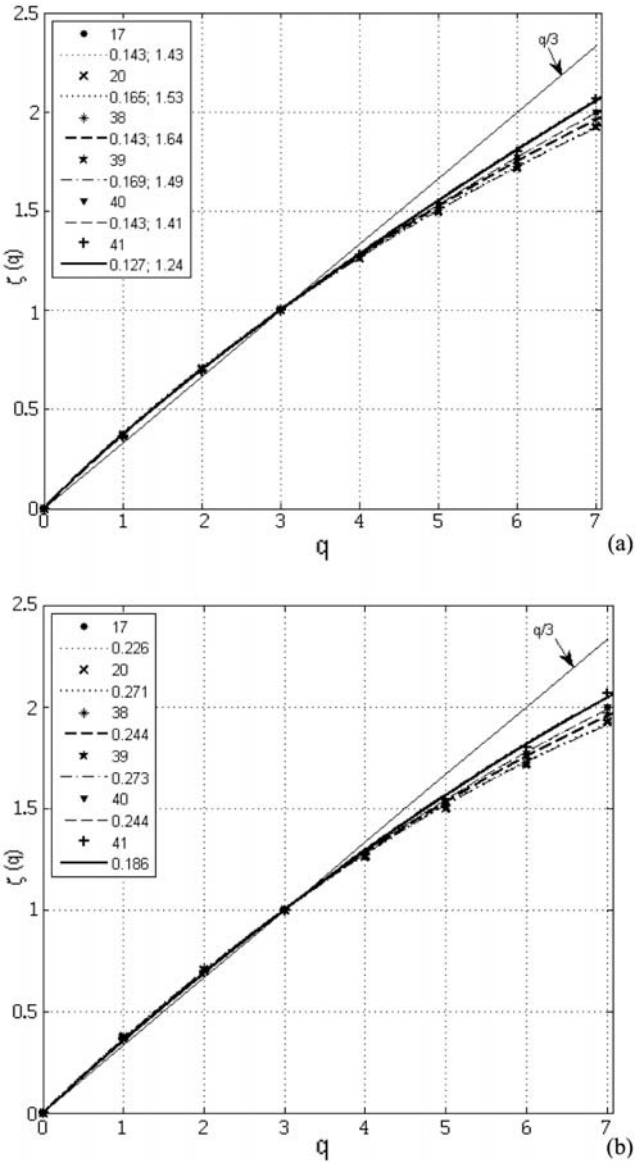

Figure 8. The scaling exponents $\xi(q)$ for q = 1–7 for segments with the highest Re_{nb}. The (a) multifractal (equation (5)) and (b) lognormal (equation (6)) model approximations are shown. The segment numbers (17–41) and the corresponding model parameters (C_1 and α (Figure 8a) and μ (Figure 8b)) are given in the insets.

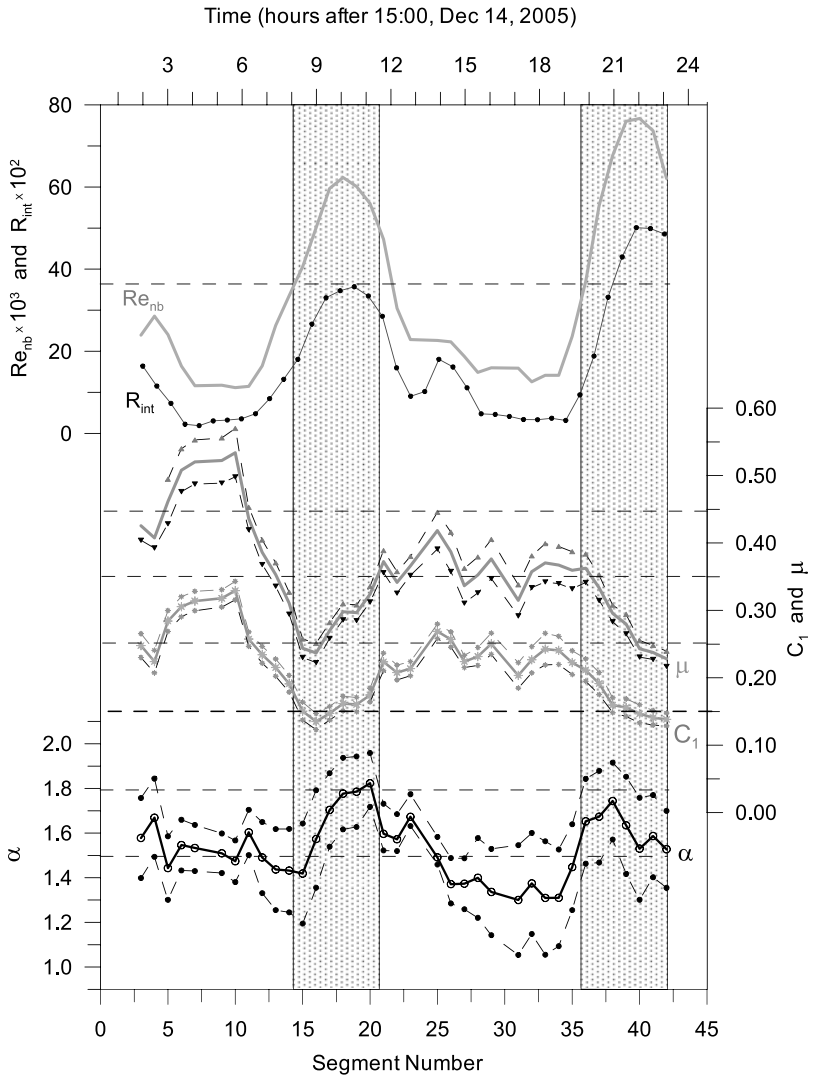

Figure 9. Parameters of the multifractal (equation (5), C_1 and α) and lognormal (equation (6), μ) intermittency models. The near-bottom (Re_{nb}) and integral turbulent (R_{int}) Reynolds numbers are mainly in phase with α and out of phase with C_1 and μ. The intermittency parameters are shown with 95% confidence bounds. Two periods of flooding current with highest Re_{nb} and R_{int} recorded are highlighted.

with the highest integral turbulent Reynolds number R_{int} (Figure 8)

$$R_{int} = rms\left(w'\right)L_{int}/\nu, \tag{13}$$

where L_{int} is given in equation (10), the scaling exponents yield the mean and the *rms* boundaries of the codimension parameter $\widetilde{C}_1 = 0.148 \pm 0.016$ and the Levy parameter $\widetilde{\alpha} = 1.46 \pm 0.13$. Both are in good agreement with the "universal" values $\hat{C}_1 = 0.15$ and $\hat{\alpha} = 1.5$ obtained in previous high Reynolds number laboratory and atmospheric measurements cited in section 2.

[32] At the segments with low R_{int} (segments 5, 13, 23, 29 in Figure 7a), the scaling exponents $\xi_i(q)$ substantially depart from the classic function $\xi_i(q) = q/3$, demonstrating an amplification of C_1 compared to $\widetilde{C}_1$. This tendency is not monotonic, and at few segments with low Re_{int}, C_1 was also low (e.g., segments 28 and 31 not shown in Figure 7a).

[33] The lognormal approximation (equation (6)) of the same experimental $\xi_i(q)$ functions yielded high-confidence fits (Figures 7b and 8b). The intermittency parameter μ followed the variations of C_1, generally out of phase with Re_{nb} and R_{int} (see Figure 9). In section 2, it was mentioned that a universal value of $\hat{\mu} \sim 0.25$ is expected [*Sreenivasan and Kailasnath*, 1993] in well-developed high Reynolds number turbulent flows. For the highest Re_{int} segments, the scaling exponents follow the lognormal intermittency model with a mean $\widetilde{\mu} = 0.237 \pm 0.033$ (Figure 8b), which is close to the suggested $\hat{\mu} = 0.25$. This shows that internal intermittency of turbulence during energetic tidal flow phases can be satisfactorily described by either a multifractal intermittency model or a classical lognormal model with universal intermittency parameters. In segments with moderate and low Re_{int}, μ generally exceeded $\hat{\mu}$, sometimes increasing to 0.5 or beyond (see Figure 7b), although, as in the case of C_1, this tendency is not monotonic.

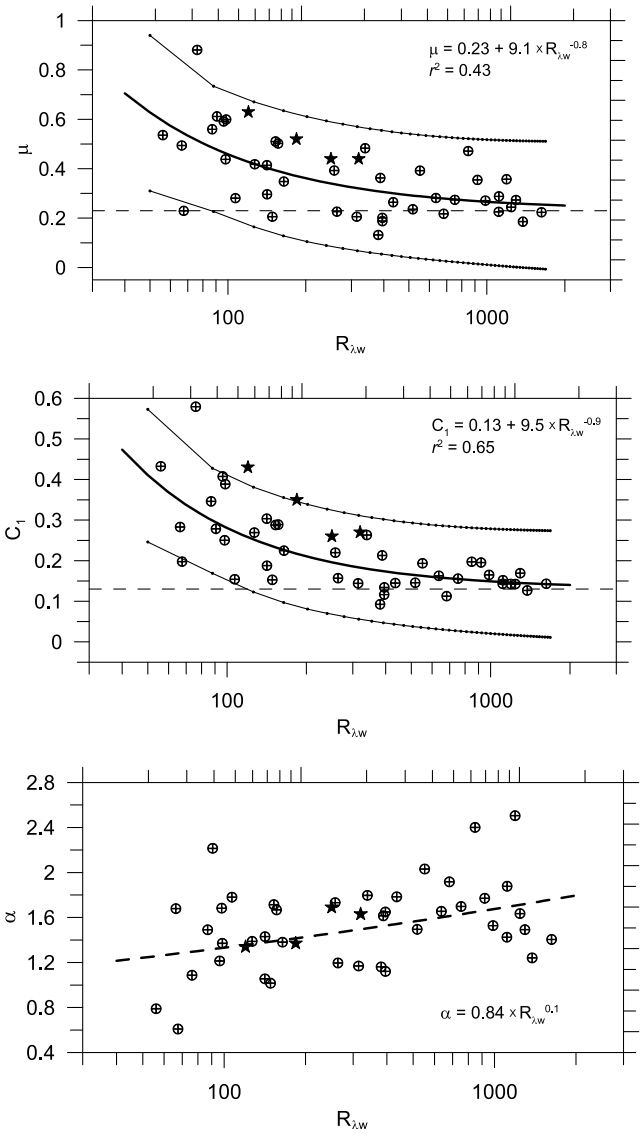

Figure 10. The dependencies of intermittency parameters μ, C_1, and α on the local turbulent Reynolds number R_{λ_w}. The least-squared fits with 95% lower and upper confident bounds (for μ and C_1) are shown. The laboratory data of *Hao et al.* [2008] are shown by stars (see text for details).

[34] The running average of the intermittency parameters shown in Figure 9 indicate that the temporal variations of μ, C_1 and α are all affected by the semidiurnal tidal cycle and seiching, which is evident from temporal variations of Re_{nb} and Re_{int}.

5.4. Dependence on the Turbulent Reynolds Number $R_{\lambda w}$

[35] In order to illustrate the dependence of μ, C_1, and α on internal flow parameters, they are plotted in Figure 10 as a function of the microscale Reynolds number $R_{\lambda w}$ (equation (11)), which is a variant of $R_\lambda = rms(u')\lambda/\nu$. This modification, however, precludes direct comparison of our results with most laboratory experiments, where R_λ is specified. Despite high scatter, the data show a general increase of μ and C_1 with decreasing $R_{\lambda w}$ (Figures 10 (top) and 10 (middle)). The best least squares power trends are given with 95% confidence bounds and the coefficients of determination r^2. The empirical functions so obtained are

$$\mu = 0.23 + R_{\lambda w}^{-0.8} \quad \text{and} \quad C_1 = 0.13 + R_{\lambda w}^{-0.9}, \tag{14}$$

implying that μ and C_1 have similar dependencies on $R_{\lambda w}$, attaining asymptotic values $\mu^o = 0.23$ and $C_1^o = 0.13$ at high $R_{\lambda w} > 500$–700. Both estimates are close to the universal values of $\hat{\mu}$ and $\hat{C}_1$ expected from turbulence intermittency models at high Reynolds numbers. A weak (statistically insignificant) dependence of α on $R_{\lambda w}$ is shown in Figure 10 (bottom). The mean value of α, $\widetilde{\alpha} = 1.53 \pm 0.39$, however, matches well with the universal $\hat{\alpha} = 1.5$–1.55 cited by *Seuront et al.* [2005] for log-Levy multifractal intermittency model. It should be reminded that the analysis here was based on TSF.

[36] Qualitatively similar dependence of $\xi_i(q)$ on R_λ has been reported by *Hao et al.* [2008, Figure 6] for TSF. These authors, however, found that the scaling exponents for the longitudinal structure functions are independent of R_λ. In order to compare laboratory findings with our results, Figure 6 of *Hao et al.* [2008] was digitized, wherein the scaling exponent $\xi(q = 0$–$8)$ of TSF is shown for $R_\lambda = 120$, 184, 250, and 350. The empirical functions $\xi(q)$ were then approximated by multifractal (equation (5)) and lognormal (equation (6)) intermittency models. The resulting intermittency parameters are shown in Figure 10 by stars. The laboratory and field data agreed well in the range of the variability of μ and α. We conclude that the oceanographic and laboratory measurements of TSF show an increasing tendency *of* intermittency parameters with decreasing $R_{\lambda w}$, which is evident from Figure 10.

5.5. Scaling Exponent of Second-Order SF as a Function of $R_{\lambda w}$

[37] As pointed out before, refined similarity hypothesis (RSH) suggests that spectral densities of velocity components and the corresponding second-order SF must deviate in the inertial subrange from the classic "−5/3" and "2/3" laws, respectively, due to internal intermittency. If the intermittency parameters C_1 and μ are dependent on $R_{\lambda w}$ at relatively low $R_{\lambda w} < 500$–700 (equation (14)), then the scaling exponent of the second-order SF $\xi(2)$ can be a function of $R_{\lambda w}$ as well. Based on the concept of incomplete self-similarity, *Barenblatt* [1996] showed that the limiting behavior of the first moments of the velocity field takes the form of an inverse logarithmic dependence on the Reynolds number [see also *Barenblatt et al.*, 1999; *Barenblatt and Chorin*, 2004]. Therefore, the higher moments are expected to converge to a limit at the same or a lower rate with increasing *Re*. For the second-order structure function $S^{(q=2)}$, the following formula has been suggested [*Barenblatt and Goldenfeld*, 1995; *Barenblatt et al.*, 1999]

$$S^{(q=2)}(r) = (\widetilde{\varepsilon} r)^{2/3}\left(c_0 + \frac{c_{01}}{\ln Re}\right)\left(\frac{r}{\eta}\right)^{\gamma_1/\ln Re}, \tag{15}$$

where c_0, c_{01}, and γ_1 are constants, and $\ln Re \equiv \log Re$ is the natural logarithm of a Reynolds number *Re*. If *Re* is taken as $R_{\lambda w}$ and empirical values of $S^{(q=2)}$ exponent $\xi_i(2)$ are plotted against $\log R_{\lambda w}$, then a decreasing trend of $\xi(2)$ is well evident with increase of $\log R_{\lambda w}$ (see

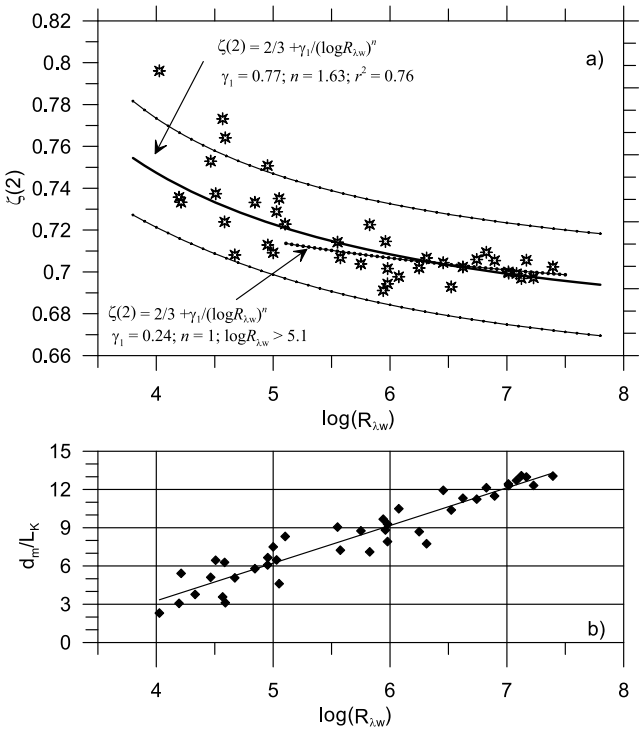

Figure 11. (a) Scaling exponent of the second-order TSF $\zeta(2)$ as a function of the natural logarithm of local turbulent Reynolds number log R_{λ_w} approximated by equation (15) (dotted line) using the adjustable parameter of equation (16) $\gamma_1 = 0.24$ (25 samples for log $R_{\lambda_w} > 5.1$). A modification for this formula (with $n = 1.63$ and $\gamma_1 = 0.77$) was applied to the entire R_{λ_w} variability (bold line). (b) The ratio between the "Taylor separation distance" $d_m = U\tau_\eta$ and $L_K = 15\eta$, where $\eta = (\nu^3/\widetilde{\varepsilon})^{1/4}$ and $\tau_\eta = (\nu/\widetilde{\varepsilon})^{1/2}$ are the Kolmogorov length and time scales, respectively, and U the mean velocity for each segment.

Figure 11a). In the spirit of equation (15), this trend could be approximated as

$$\xi(2) = \exp\left[S^{(q=2)}\right] = 2/3 + \gamma_1/(\log R_{\lambda w})^n. \qquad (16)$$

The least squared fit of equation (16) to data gave $\gamma_1 = 0.77$ and $n = 1.63$ with $r^2 = 0.76$ for the entire range of log $R_{\lambda w}$ variability (log $R_{\lambda w}$ = 4–7.5). The rate of increase of $\xi(2)$ at low $R_{\lambda w}$ is substantially higher than the inverse logarithmic rate that equation (15) predicts. If only high $R_{\lambda w}$ are considered and the approximation (16) with $n = 1$ is enforced for log $R_{\lambda w} > \sim 5.1$ ($R_{\lambda w} > 150$), the inverse logarithmic function fits the data reasonably well with $\gamma_1 = 0.24$.

6. Discussion

6.1. Universality of $\xi(2)$

[38] The behavior of $\xi(2)$ at low Reynolds numbers suggested by *Barenblatt and Goldenfeld* [1995] appears to be born out by our data, but the rate of increase is not in par with that predicted by the inverse logarithmic rate (equation (15)). Note that the 2/3 power law for $\xi(2)$ is expected only at very high $R_{\lambda w}$. For the range of Reynolds numbers considered in this paper, $\xi(2)$ somewhat exceeded 2/3 and was close to 0.7 for log $R_{\lambda w} > 6$, which is consistent with the laboratory results of *Benzi et al.* [1995]. *Benzi et al.* [1999] also concluded that the universal (Reynolds number independent) value of $\xi(2)$ is close to 0.7 rather than 2/3. This assertion is not supported by the presented data, which show the possibility of further reduction of $\xi(2)$ toward classical 2/3 at very high $R_{\lambda w}$.

6.2. Test of Taylor Hypothesis

[39] Our analysis of turbulence intermittency in a tidal BBL and several laboratory experiments [e.g., *Shen and Warhaft*, 2000; *Pearson and Antonia*, 2001; *Cleve et al.*, 2004; *Arenas and Chorin*, 2006; *Hao et al.*, 2008] have shown that $\xi(q)$ is a function of *Re*. The *Re* dependence of $\xi(q)$, however, has been disputed [e.g., *Benzi et al.*, 1999; *Castaing*, 2006] mainly on the basis that Taylor hypothesis may fail at low R_λ by introducing a bias to SF exponents. Responding to the concern of *Castaing* [2006], *Sreenivasan* [2006] questioned whether the relationship between $\xi(q)$ and R_λ can be affected by Taylor hypothesis, calling for direct and accurate spatial turbulent measurements to resolve the concern. To our knowledge, no such measurements exist, but the numerical simulations on SF without using Taylor hypothesis [e.g., *Briscolini et al.*, 1994] have confirmed the applicability of ESS in flows with R_λ as low as 32.

[40] Although the $rms_i(w')$ in the tidal flow never exceeded several percents of the mean advection velocity U_i, we decided to study the influence of Taylor hypothesis on our data by running an additional test recommended by *Castaing* [2006]. Restricting frozen turbulence hypothesis to the Kolmogorov time scale $\tau_\eta = (\nu/\widetilde{\varepsilon})^{1/2}$, *Castaing* [2006] suggested that the "Taylor separation distance" $d_m = U\tau_\eta$ must exceed the dissipation scale ($L_K = 15\eta$) in order to develop a reasonable linear range in SF. Using our measurements, the ratio d_m/L_K was calculated for each data segment by employing spectrally obtained estimates of the mean dissipation rate $\widetilde{\varepsilon}$. The ratio d_m/L_K is shown in Figure 11b as a function of log($R_{\lambda w}$), which can be inspected vis-à-vis the plot of $\xi(2)$ versus log($R_{\lambda w}$) in Figure 11a. For log($R_{\lambda w}$) > 5, the results show $d_m/L_K > 6$, suggesting that even for not very high turbulent Reynolds numbers Taylor hypothesis should work well ($R_{\lambda w} > 150$). As such, the weak inverse logarithmic dependence of $\xi(2)$ on $R_{\lambda w}$ observed for log(R_{λ_w}) > 5 can be accepted with confidence. The samples of $\xi(2)$ at log($R_{\lambda w}$) < 5, which show a faster increase of the scaling exponent with decreasing $R_{\lambda w}$, were in the range $3 < d_m/L_K < 6$, which is not sufficient to invalidate Taylor hypothesis. The break of $\xi(2)$ behavior observed at log($R_{\lambda w}$) $\approx$ 5, nevertheless, raises concerns of whether there is a breakdown of Taylor hypothesis when log($R_{\lambda w}$) < 5.

6.3. Influence of Anisotropy and the Nature of the Flow

[41] The scaling exponents of TSF can be differently affected by the Reynolds number compared to those of the longitudinal SF due to anisotropy, which was found in some laboratory studies [*Antonia et al.*, 2002]. The nature of the flow may also influence the $R_{\lambda w}$ dependence of $\xi(q)$ and intermittency model parameters. For example, in the oceans, the intermittency in a reversing highly sheared tidal flow over the seabed (current case) may have different scaling compared to wave-generated turbulence, flow near the sea surface (drift currents), currents around and behind obstacles

(seamounts), parallel shear and jets flows (equatorial counter currents) and river plumes. After all, large-scale structures of these flows are different, and the assumption was made that the selected averaging period was appropriate to analyze only the universal turbulent structures and energy cascade. The use of isotropic assumption in calculation of the dissipation rate instead of utilizing the full three-dimensional energy dissipation tensor [e.g., *Hosokawa et al.*, 1996; *Wang et al.*, 1996] may affect $R_{\lambda w}$ and R_λ calculations, and hence the dependence of $\xi(q)$ on corresponding Reynolds numbers. All these factors may influence specific forms of the scaling laws given by equations (14) and (16), but the tendencies of increasing μ, C_1, and $\xi(2)$ with decreasing $R_{\lambda w}$ is expected to hold. The intermittency parameters and the scaling exponent of the second-order SF approach their universal asymptotic values at very high Reynolds numbers.

7. Conclusions

[42] The ADV measurements of vertical velocity (w) in a tidal current on a shallow shelf of the East China Sea were used to calculate higher-order transverse structure functions (TSF) in the streamwise direction, based on which the intermittency characteristics of turbulence near the seafloor were studied. It was found that at fairly low Reynolds numbers Re the TSF scaling exponents $\xi(q)$ (with respect to the third-order TSF) progressively deviate from the classical universal turbulent regime $\xi(q) = q/3$ as Re decreases, possibly due to higher intermittency of underdeveloped turbulence. The second-order TSF scaling exponent $\xi(2)$ shows an inverse logarithm dependence on the microscale turbulent Reynolds number $R_{\lambda w}$ for $R_{\lambda w} > 150$, supporting the theoretical formulation of *Barenblatt and Goldenfeld* [1995].

[43] The application of the classical single-parameter (μ) lognormal model and two-parameter (C_1 and α) log-Levy multifractal model for scaling of SF exponents $\xi(q)$ shows that during high-speed flooding phases of tidal flow the mean intermittency parameters are $\widetilde{\mu} \approx 0.24$, $\widetilde{C}_1 \approx 0.15$, and $\widetilde{\alpha} \approx 1.5$. These are close to the canonical universal values for well-developed turbulence at high Reynolds numbers. When the turbulent Reynolds number $R_{\lambda w}$ drops below ~100, μ and C_1, showed a tendency to increase up to $\mu \sim 0.5$–0.6 and $C_1 \sim 0.25$–0.35.

[44] The relationships between μ, C_1 and $R_{\lambda w}$ were approximated by power law functions (equation (14)) with asymptotic values of $\mu^o = 0.23$ and $C_1^o = 0.13$ at very high Reynolds numbers. The dependence of intermittency parameters on Reynolds number delineated in this study helps to resolve the controversy between small universal values of μ and C_1 obtained previously in high Reynolds number laboratory and atmospheric flows and relatively large values of $\mu = 0.4$–0.5 reported for stratified ocean turbulence [*Baker and Gibson*, 1987; *Gibson*, 1991; *Fernando and Lozovatsky*, 2001]. Note that turbulent patches in the pycnocline are usually associated with relatively low $R_{\lambda w}$. The dependence of intermittency parameters on microscale Reynolds number obtained in laboratory experiments of *Hao et al.* [2008] is in general agreement with the results of the present study for tidally induced turbulence in the marine bottom boundary layer. The influence of Reynolds number R_λ on the scaling exponents of transverse and longitudinal structure functions is expected to depend on the nature of the flow and anisotropy of turbulence, which must be addressed in future studies. Small-scale as well as mesoscale intermittencies of turbulence in natural waters should be taken into account in developing new parameterizations of vertical and lateral mixing for advance numerical models of oceanic and atmospheric dynamics.

[45] **Acknowledgments.** This study was supported by the U.S. Office of Naval Research (grant N00014-05-1-0245), the Spanish Ministry of Education and Science (grant FIS2008-03608), and the Major State Program of China for Basic Research (grant 2006CB400602). The first author also received financial support during his temporary affiliation with the Catalan Institute for Water Research (ICRA).

References

Anselmet, F., R. A. Antonia, and L. Danailaa (2001), Turbulent flows and intermittency in laboratory experiments, *Planet. Space Sci.*, *49*, 1177–1191, doi:10.1016/S0032-0633(01)00059-9.

Antonia, R. A., T. Zhou, and G. P. Romano (2002), Small-scale turbulence characteristics of two-dimensional bluff body wakes, *J. Fluid Mech.*, *459*, 67–92, doi:10.1017/S0022112002007942.

Arenas, A., and A. J. Chorin (2006), On the existence and scaling of structure functions in turbulence according to the data, *Proc. Natl. Acad. Sci. U. S. A.*, *103*, 4352–4355, doi:10.1073/pnas.0600482103.

Baker, M. A., and C. H. Gibson (1987), Sampling turbulence in the stratified ocean: Statistical consequences of strong intermittency, *J. Phys. Oceanogr.*, *17*, 1817–1837, doi:10.1175/1520-0485(1987)017<1817:STITSO>2.0.CO;2.

Barenblatt, G. I. (1996), *Similarity, Self-Similarity, and Intermediate Asymptotics*, 386 pp., Cambridge Univ. Press, Cambridge, U. K.

Barenblatt, G. I., and A. J. Chorin (2004), A mathematical model for the scaling of turbulence, *Proc. Natl. Acad. Sci. U. S. A.*, *101*, 15,023–15,026, doi:10.1073/pnas.0406291101.

Barenblatt, G. I., and N. D. Goldenfeld (1995), Does fully developed turbulence exist? Reynolds number independence versus asymptotic covariance, *Phys. Fluids*, *7*, 3078–3082, doi:10.1063/1.868685.

Barenblatt, G. I., A. J. Chorin, and V. M. Prostokishin (1999), Comment on the paper "On the scaling of three-dimensional homogeneous and isotropic turbulence" by Benzi et al., *Physica D*, *127*, 105–110, doi:10.1016/S0167-2789(98)00289-9.

Benzi, R., S. Ciliberto, R. Tripiccione, C. Baudet, F. Massaioli, and S. Succi (1993), Extended self similarity in turbulent flows, *Phys. Rev. E*, *48*, R29–R32, doi:10.1103/PhysRevE.48.R29.

Benzi, R., S. Ciliberto, C. Baudet, and G. Ruiz Chavarria (1995), On the scaling of three-dimensional homogeneous and isotropic turbulence, *Physica D*, *80*, 385–398, doi:10.1016/0167-2789(94)00190-2.

Benzi, R., S. Ciliberto, C. Baudet, and G. Ruiz-Chavarria (1999), Reply to the comment of Barenblatt et al., *Physica D*, *127*, 111–112, doi:10.1016/S0167-2789(98)00290-5.

Bowers, D. G., and J. H. Simpson (1987), Mean position of tidal fronts in European-shelf seas, *Cont. Shelf Res.*, *7*, 35–44, doi:10.1016/0278-4343(87)90062-8.

Briscolini, M., P. Santangelo, S. Succi, and R. Benzi (1994), Extended self similarity in the numerical simulation of three dimensional homogeneous flows, *Phys. Rev. E*, *50*, R1745–R1747.

Camussi, R., D. Barbagallo, G. Guj, and F. Stella (1996), Transverse and longitudinal scaling laws in non-homogeneous low *Re* turbulence, *Phys. Fluids*, *8*, 1181–1191, doi:10.1063/1.868909.

Castaing, B. (2006), Comment on "Intermittency exponent of the turbulent energy cascade", *Phys. Rev. E*, *73*, 068301.1, doi:10.1103/PhysRevE.73.068301.

Cleve, J., M. Greiner, B. R. Pearson, and K. R. Sreenivasan (2004), Intermittency exponent of the turbulent energy cascade, *Phys. Rev. E*, *69*, 066316.1–066316.6, doi:10.1103/PhysRevE.69.066316.

Colosi, J. A., et al. (1999), A review of recent results on ocean acoustic wave propagation in random media: Basin scales, *IEEE J. Oceanic Eng.*, *24*, 138–155, doi:10.1109/48.757267.

Davis, R. E. (1996), Sampling turbulent dissipation, *J. Phys. Oceanogr.*, *26*, 341–358, doi:10.1175/1520-0485(1996)026<0341:STD>2.0.CO;2.

Druet, C. (2003), The fine structure of marine hydrophysical fields and its influence on the behavior of plankton: An overview of some experimental and theoretical investigations, *Oceanologia*, *45*(4), 517–555.

Feller, W. (1971), *An Introduction to Probability Theory and Its Applications*, vol. 2, 2nd ed., 683 pp., Wiley, New York.

Fernando, H. J. S., and I. D. Lozovatsky (2001), Turbulence and mixing in oceans, in *Proceedings of the 6th Workshop on Physical Processes in Natural Waters*, edited by X. Casamitjana, pp. 1–13, Univ. de Girona, Girona, Spain.

Fournier, J.-D., and U. Frisch (1978), *d*-dimensional turbulence, *Phys. Rev. A*, *17*, 747–762, doi:10.1103/PhysRevA.17.747.

Frisch, U. (1995), *Turbulence: The Legacy of A. N. Kolmogorov*, 296 pp., Cambridge Univ. Press, Cambridge, U. K.

Gibson, C. H. (1981), Buoyancy effects in turbulent mixing: Sampling turbulence in the stratified ocean, *AIAA J.*, *19*, 1394–1400, doi:10.2514/3.60076.

Gibson, C. H. (1991), Kolmogorov similarity hypotheses for scalar fields: Sampling intermittent turbulent mixing in the ocean and galaxy, *Proc. R. Soc. London Ser. A*, *434*, 149–164, doi:10.1098/rspa.1991.0086.

Gibson, C. H. (1998), Intermittency of internal wave shear and turbulence dissipation, in *Physical Processes in Lakes and Oceans*, *Coastal Estuarine Stud.*, vol. 54, edited by J. Imberger, pp. 363–376, AGU, Washington, D. C.

Gibson, C. H., G. R. Stegen, and S. McConnell (1970), Measurements of the universal constant in Kolmogoroff's third hypothesis for high Reynolds number turbulence, *Phys. Fluids*, *13*(10), 2448–2451, doi:10.1063/1.1692811.

Goring, D. G., and V. I. Nikora (2002), Despiking acoustic Doppler velocimeter records, *J. Hydraul. Eng.*, *128*, 117–126, doi:10.1061/(ASCE)0733-9429(2002)128:1(117).

Gregg, M. C., H. E. Seim, and D. B. Percival (1993), Statistics of shear and turbulent dissipation profiles in random internal wave fields, *J. Phys. Oceanogr.*, *23*, 1777–1799, doi:10.1175/1520-0485(1993)023<1777:SOSATD>2.0.CO;2.

Gregg, M. C., D. P. Winkel, T. B. Sanford, and H. Peters (1996), Turbulence produced by internal waves in the oceanic thermocline at mid and low latitudes, *Dyn. Atmos. Oceans*, *24*, 1–14, doi:10.1016/0377-0265(95)00406-8.

Gurvich, A. S., and A. M. Yaglom (1967), Breakdown of eddies and probability distributions for small-scale turbulence, *Phys. Fluids*, *10*, suppl., S59–S65, doi:10.1063/1.1762505.

Hao, Z., T. Zhou, Y. Zhou, and J. Mi (2008), Reynolds number dependence of the inertial range scaling of energy dissipation rate and enstrophy in a cylinder wake, *Exp. Fluids*, *44*, 279–289, doi:10.1007/s00348-007-0400-5.

Hosokawa, I., S. I. Oide, and K. Yamamoto (1996), Isotropic turbulence: Important differences between true dissipation rate and its one-dimensional surrogate, *Phys. Rev. Lett.*, *77*, 4548–4551, doi:10.1103/PhysRevLett.77.4548.

Kolmogorov, A. N. (1941a), The local structure of turbulence in incompressible fluid for very large Reynolds numbers (in Russian), *Dokl. Acad. Sci. USSR*, *30*(4), 299–303.

Kolmogorov, A. N. (1941b), On log-normal distribution of the sizes of particle in the course of breakdown (in Russian), *Dokl. Acad. Sci. USSR*, *31*(2), 99–101.

Kolmogorov, A. N. (1941c), On decay of isotropic turbulence in incompressible viscid fluid (in Russian), *Dokl. Acad. Sci. USSR*, *31*(6), 538–541.

Kolmogorov, A. N. (1962), A refinement of previous hypotheses concerning the local structure of turbulence in a viscous incompressible fluid at high Reynolds number, *J. Fluid Mech.*, *13*, 82–85, doi:10.1017/S0022112062000518.

Kuo, A. Y.-C., and S. Corrsin (1971), Experiments on internal intermittency and fine-structure distribution functions in fully turbulent fluid, *J. Fluid Mech.*, *50*(2), 285–319, doi:10.1017/S0022112071002581.

Lesieur, M. (1990), *Turbulence in Fluids: Stochastic and Numerical Modeling*, 412 pp., Kluwer Acad., Dordrecht, Netherlands.

Lovejoy, S., and D. Schertzer (2007), Scale, scaling and multifractals in geophysics: Twenty years on, in *Nonlinear Dynamics in Geosciences*, edited by A. A. Tsonis and J. Elsner, pp. 311–337, Springer, New York.

Lozovatsky, I. D., and H. J. S. Fernando (2002), Turbulent mixing on a shallow shelf of the Black Sea, *J. Phys. Oceanogr.*, *32*, 945–956, doi:10.1175/1520-0485(2002)032<0945:MOASSO>2.0.CO;2.

Lozovatsky, I. D., A. S. Ksenofontov, A. Y. Erofeev, and C. H. Gibson (1993), Modeling of the evolution of vertical structure in the upper ocean influenced by atmospheric forcing and intermittent turbulence in the pycnocline, *J. Mar. Syst.*, *4*, 263–273, doi:10.1016/0924-7963(93)90013-C.

Lozovatsky, I. D., E. Roget, H. J. S. Fernando, M. Figueroa, and S. Shapovalov (2006), Sheared turbulence in a weakly stratified upper ocean, *Deep Sea Res. Part I*, *53*, 387–407, doi:10.1016/j.dsr.2005.10.002.

Lozovatsky, I. D., Z. Liu, H. Wei, and H. J. S. Fernando (2008a), Tides and mixing in the northwestern East China Sea. Part I: Rotating and reversing tidal flows, *Cont. Shelf Res.*, *28*, 318–337, doi:10.1016/j.csr.2007.08.006.

Lozovatsky, I. D., Z. Liu, H. Wei, and H. J. S. Fernando (2008b), Tides and mixing in the northwestern East China Sea. Part II: The near-bottom turbulence, *Cont. Shelf Res.*, *28*, 338–350, doi:10.1016/j.csr.2007.08.007.

MacKenzie, B. R., and W. C. Leggett (1993), Wind-based models for estimating the dissipation rates of turbulence energy in aquatic environments: Empirical comparisons, *Mar. Ecol. Prog. Ser.*, *94*, 207–216, doi:10.3354/meps094207.

Mandelbrot, B. B. (1974), Intermittent turbulence in self-similar cascades: Divergence of high moments and dimension of the carrier, *J. Fluid Mech.*, *62*, 331–358, doi:10.1017/S0022112074000711.

Mandelbrot, B. B. (1983), *The Fractal Geometry of Nature*, 468 pp., W. H. Freeman, New York.

Margalef, R. (1985), Introduction to the Mediterranean, in *Western Mediterranean*, edited by R. Margalef, pp. 1–16, Pergamon, Oxford, U. K.

Margalef, R. (1997), *Our Biosphere*, 176 pp., Ecol. Inst., Luhe, Germany.

Mellor, G. L., and T. Yamada (1982), Development of a turbulence closure model for geophysical fluid problems, *Rev. Geophys. Space Phys.*, *20*, 851–875, doi:10.1029/RG020i004p00851.

Monin, A. S., and A. M. Yaglom (1975), *Statistical Fluid Mechanics: Mechanics of Turbulence*, vol. 2, 874 pp., MIT Press, Cambridge, Mass.

Novikov, E. A. (1970), Intermittency and scale similarity in the structure of a turbulent flow, *J. Appl. Math. Mech.*, *35*, 266–277.

Novikov, E. A. (1990), The effects of intermittency on statistical characteristics of turbulence and scale similarity of breakdown coefficients, *Phys. Fluids A*, *2*, 814–820, doi:10.1063/1.857629.

Oboukhov, A. M. (1962), Some specific features of atmospheric turbulence, *J. Fluid Mech.*, *13*, 77–81, doi:10.1017/S0022112062000506.

Pearson, B. R., and R. A. Antonia (2001), Reynolds-number dependence of turbulent velocity and pressure increments, *J. Fluid Mech.*, *444*, 343–382, doi:10.1017/S0022112001005511.

Peters, F., and C. Marrasé (2000), Effects of turbulence on plankton: An overview of experimental evidence and some theoretical considerations, *Mar. Ecol. Prog. Ser.*, *205*, 291–306, doi:10.3354/meps205291.

Pozdinin, V. D. (2002), *Small-Scale Turbulence in the Ocean* (in Russian), 202 pp., Nauka, Moscow.

Rehmann, C. R., and T. F. Duda (2000), Diapycnal diffusivity inferred from scalar microstructure measurements near the New England shelf/slope front, *J. Phys. Oceanogr.*, *30*, 1354–1371, doi:10.1175/1520-0485(2000)030<1354:DDIFSM>2.0.CO;2.

Roget, E., I. Lozovatsky, X. Sanchez, and M. Figueroa (2006), Microstructure measurements in natural waters: Methodology and applications, *Prog. Oceanogr.*, *70*, 123–148, doi:10.1016/j.pocean.2006.07.003.

Sánchez, X., and E. Roget (2007), Microstructure measurements and heat flux calculations of a triple-diffusive process in a lake within the diffusive layer convection regime, *J. Geophys. Res.*, *112*, C02012, doi:10.1029/2006JC003750.

Schertzer, D., and S. Lovejoy (1987), Physical modeling and analysis of rain clouds by anisotropic scaling multiplicative processes, *J. Geophys. Res.*, *92*, 9693–9714, doi:10.1029/JD092iD08p09693.

Seuront, L., and F. Schmitt (2001), Describing intermittent processes in the ocean—Univariate and bivariate multiscaling procedures, in *Stirring and Mixing in a Stratified Ocean: Proceedings of "Aha Huliko"a Hawaiian Winter Workshop*, edited by P. Muller and C. Garrett, pp. 129–144, Sch. of Ocean and Earth Sci. and Technol., Univ. of Hawaii at Manoa, Manoa, Hawaii.

Seuront, L., and F. G. Schmitt (2005), Multiscaling statistical procedures for the exploration of biophysical couplings in intermittent turbulence. Part II. Applications, *Deep Sea Res. Part II*, *52*, 1325–1343, doi:10.1016/j.dsr2.2005.01.005.

Seuront, L., F. Schmitt, Y. Lagadeuc, D. Schertzer, and S. Lovejoy (1999), Universal multifractal analysis as a tool to characterize multiscale intermittent patterns: Example of phytoplankton distribution in turbulent coastal waters, *J. Plankton Res.*, *21*, 877–922, doi:10.1093/plankt/21.5.877.

Seuront, L., F. Schmitt, and Y. Lagadeuc (2001), Turbulence intermittency, small-scale phytoplankton patchiness and encounter rates in plankton: Where do we go from here?, *Deep Sea Res. Part I*, *48*, 1199–1215, doi:10.1016/S0967-0637(00)00089-3.

Seuront, L., V. Gentilhomme, and Y. Lagadeuc (2002), Small-scale nutrient patches in tidally mixed coastal waters, *Mar. Ecol. Prog. Ser.*, *232*, 29–44, doi:10.3354/meps232029.

Seuront, L., H. Yamazaki, and F. G. Schmitt (2005), Intermittency, in *Marine Turbulence: Theories, Observations and Models*, edited by H. Baumert, J. Sündermann, and J. Simpson, pp. 66–78, Cambridge Univ. Press, Cambridge, U. K.

Shen, X., and Z. Warhaft (2000), The anisotropy of the small scale structure in high Reynolds number ($R_\lambda > 1000$) turbulent shear flow, *Phys. Fluids*, *12*, 2976–2989, doi:10.1063/1.1313552.

Squires, K. D., and H. Yamazaki (1995), Preferential concentration of marine particles in isotropic turbulence, *Deep Sea Res. Part I*, *42*, 1989–2004, doi:10.1016/0967-0637(95)00079-8.

Squires, K. D., and H. Yamazaki (1996), Addendum to the paper "Preferential concentration of marine particles in isotropic turbulence", *Deep Sea Res. Part I*, *43*, 1865–1866, doi:10.1016/S0967-0637(96)00085-4.

Sreenivasan, K. R. (1995), On the universality of the Kolmogorov constant, *Phys. Fluids*, *7*, 2778–2784, doi:10.1063/1.868656.

Sreenivasan, K. R. (2004), Possible effects of small-scale intermittency in turbulent reacting flows, *Flow Turbul. Combus.*, *72*(2–4), 115–131, doi:10.1023/B:APPL.0000044408.46141.26.

Sreenivasan, K. R. (2006), Reply to "Comment on 'Intermittency exponent of the turbulent energy cascade'", *Phys. Rev. E*, *73*, 068302.1, doi:10.1103/PhysRevE.73.068302.

Sreenivasan, K. R., and R. A. Antonia (1997), The phenomenology of small-scale turbulence, *Annu. Rev. Fluid Mech.*, *29*, 435–472, doi:10.1146/annurev.fluid.29.1.435.

Sreenivasan, K. R., and P. Kailasnath (1993), An update on the intermittency exponent in turbulence, *Phys. Fluids A*, *5*, 512–514, doi:10.1063/1.858877.

Stapleton, K. R., and D. A. Huntley (1995), Seabed stress determination using the inertial dissipation method and the turbulent kinetic energy method, *Earth Surf. Processes Landforms*, *20*, 807–815, doi:10.1002/esp.3290200906.

Tennekes, H., and J. L. Lumley (1972), *A First Course in Turbulence*, 300 pp., MIT Press, Cambridge, Mass.

Tsinober, A. (2001), *An Informal Introduction to Turbulence*, 324 pp., Kluwer Acad., New York.

Tyson, R. K. (1991), *Principles of Adaptive Optics*, 298 pp., Academic, San Diego, Calif.

van de Water, W., and J. A. Herweijer (1999), High-order structure functions of turbulence, *J. Fluid Mech.*, *387*, 3–37, doi:10.1017/S0022112099004814.

Vassilicos, J. C. (2001), *Intermittency in Turbulent Flows*, 276 pp., Cambridge Univ. Press, Cambridge, U. K.

Voulgaris, G., and J. H. Trowbridge (1998), Evaluation of the Acoustic Doppler Velocimeter (ADV) for turbulence measurements, *J. Atmos. Oceanic Technol.*, *15*(1), 272–289, doi:10.1175/1520-0426(1998)015<0272:EOTADV>2.0.CO;2.

Wang, L. P., S. Chen, J. G. Brasseur, and J. C. Wyngaard (1996), Examination of hypotheses in Kolmogorov refined turbulence theory through high-resolution simulations. Part 1. Velocity field, *J. Fluid Mech.*, *309*, 113–156, doi:10.1017/S0022112096001589.

Yaglom, A. M. (1966), The influence of fluctuations of energy dissipation on the shape of turbulent characteristics in the inertial interval (in Russian), *Sov. Phys. Dokl.*, *2*, 26–29.

Yamazaki, H., and R. Lueck (1990), Why oceanic dissipation rates are not lognormal, *J. Phys. Oceanogr.*, *20*, 1907–1918, doi:10.1175/1520-0485(1990)020<1907:WODRAN>2.0.CO;2.

Yamazaki, H., J. G. Mitchell, L. Seuront, F. Wolk, and H. Li (2006), Phytoplankton microstructure in fully developed oceanic turbulence, *Geophys. Res. Lett.*, *33*, L01603, doi:10.1029/2005GL024103.

H. J. S. Fernando and I. Lozovatsky, Center for Environmental Fluid Dynamics, Department of Mechanical and Aerospace Engineering, Arizona State University, Tempe, AZ 85287-8909, USA.

Z. Liu, State Key Laboratory of Marine Environmental Science, Xiamen University, Xiamen 361005, China.

J. Planella and E. Roget, Environmental Physics Group, Department of Physics, University of Girona, Catalonia, E-17071 Girona, Spain. (elena.roget@udg.edu)